Molecular Phylogenetics and Evolution 107 (2017) 56–63

Contents lists available at ScienceDirect

Molecular Phylogenetics and Evolution

journal homepage: www.elsevier.com/locate/ympev

Review

Hidden diversity within the lizard genus *Liolaemus*: Genetic vs morphological divergence in the *L. rothi* complex (Squamata: Liolaeminae)

Melisa Olave [a,*], Luciano J. Avila [a], Jack W. Sites Jr. [b], Mariana Morando [a]

[a] Instituto Patagónico para el Estudio de los Ecosistemas Continentales – Consejo Nacional de Investigaciones Científicas y Técnicas (IPEEC-CENPAT-CONICET), Boulevard Almirante Brown 2915, ZC: U9120ACD Puerto Madryn, Chubut, Argentina
[b] Department of Biology and M.L. Bean Life Science Museum, Brigham Young University (BYU), Provo, UT 84602, USA

ARTICLE INFO

Article history:
Received 14 April 2016
Revised 25 July 2016
Accepted 12 September 2016
Available online 13 September 2016

Keywords:
Natural selection
Species tree
iBPP
Divergence times
Patagonia

ABSTRACT

Currently, *Liolaemus* is the second most species-rich reptile genus in the world (257 species), and predictions of its real diversity suggest that it may be the most diverse genus. Originally, *Liolaemus* species were described as widely distributed and morphologically variable taxa, but extensive sampling in previously unexplored geographic areas, coupled with molecular and more extensive morphological studies, have discovered an unexpectedly high number of previously undetected species.

Here, we study the level of molecular vs. morphological divergence within the *L. rothi* complex, combining a total of 14 loci (2 mitochondrial and 12 nuclear loci) for 97 individuals, as well as morphological data (nine morphometric and 15 color pattern variables), that represent all six described species of the *L. rothi* complex, plus two candidate species. We use the multi-coalescent species delimitation program iBPP and resolve strong differences in molecular divergence; and each species is inferred as an independent lineage supported by high posterior probabilities. However, morphological differences are not that clear, and our modeling of morphological characters suggests differential selection pressures implying some level of morphological stasis. We discuss the role of natural selection on phenotypic traits, which may be an important factor in "hiding" the real diversity of the genus.

Contents

1. Introduction . . . 57
2. Material and methods . . . 57
   2.1. Field sampling . . . 57
   2.2. Laboratory procedures . . . 57
   2.3. Species tree estimation . . . 58
   2.4. Divergence time estimation . . . 58
   2.5. Morphological comparisons . . . 58
   2.6. Molecular and morphological species delimitation . . . 58
   2.7. Morphological evolution . . . 59
3. Results . . . 59
   3.1. Species tree and divergence times . . . 59
   3.2. Molecular and morphological divergence . . . 59
   3.3. Morphological evolution . . . 61
4. Discussion . . . 61
   4.1. Hidden diversity in the genus *Liolaemus*: genetic vs. morphological divergence . . . 61
   4.2. The *L. rothi* complex species tree . . . 62

* Corresponding author.
E-mail addresses: olave@cenpat-conicet.gob.ar (M. Olave), avila@cenpat-conicet.gob.ar (L.J. Avila), jack_sites@byu.edu (J.W. Sites Jr.), morando@cenpat-conicet.gob.ar (M. Morando).

http://dx.doi.org/10.1016/j.ympev.2016.09.009
1055-7903/

Acknowledgments 62
Appendix S1. Supplementary material 62
References 62

1. Introduction

Over the last 30 years herpetologists have focused intensive study on the temperate South American lizard genus *Liolaemus*, leading to the description of many new species. Originally, most species of *Liolaemus* were described as widely distributed and morphologically variable species (e.g., Koslowsky, 1898), but more recent molecular studies resolved large numbers of well-supported clades within widely distributed morphological species. Most of these were resolved with the mtDNA locus alone, and were identified as "candidate species" in need of further study (Morando et al., 2003). Currently, *Liolaemus* constitutes the second most species-rich reptile genus in the world (257 species; Abdala and Quinteros, 2014) but this number is considered an underestimate; some predictions suggest that it could be the most diverse genus (Morando et al., 2003). Discovering this cryptic diversity was based on extensive sampling of previously unexplored geographic areas, and incorporating molecular data (e.g., Morando et al., 2003, 2004, 2007, 2008; Avila et al., 2006; Breitman et al., 2011, 2012; Medina et al., 2014; Olave et al., 2014a; Aguilar et al., 2013). These studies were based on a conceptual "general lineage" species concept that define a species as a lineage evolving independently of other such lineages (de Queiroz, 2007). Operationally this lineage may or may not be phenotypically distinguishable, diagnosable, monophyletic, reproductively isolated, or ecologically divergent; these are empirical attributes that we may use to delimit species lineages.

In order to bring objectivity and reproducibility into species delimitation, different methodological approaches have been proposed (summarized in Camargo and Sites, 2013; Carstens et al., 2013). In particular, using molecular data for species delimitation has become popular (Knowles, 2009; Edward and Knowles, 2014) and some recently proposed options aim to identify independent evolving lineages based on DNA sequences (multiple loci) and coalescent models that delimit species without reciprocal monophyly (Yang and Rannala, 2010). Among available algorithms, the program *integrated Bayesian Phylogenetic and Phylogeography* (iBPP; Solís-Lemus et al., 2015) evaluates the posterior probabilities of species divergence. This program extends the original BPP algorithm, which analyzed sequence data only (Yang and Rannala, 2010; Rannala and Yang, 2013), by also including phenotypic data. Recent studies show that delimiting species with single sources of information, especially molecular data, has limitations and biases (Edward and Knowles, 2014; Olave et al., 2014b). The iBPP algorithm represents an advance in that morphological data can be included, and may reduce type I errors in species delimitation (Olave et al., 2014b).

Differences between molecular and phenotypic divergence may identify interesting evolutionary patterns; for example these different rates of evolutionary change could be explained by natural selection, which can be evaluated against the null hypothesis of random evolution (Harmon et al., 2008). Specifically, phenotypic change models have been proposed to explain morphological diversification within clades, such as Brownian motion (also known as "random walk"), to predict the level of morphological differentiation expected by chance along a species tree (the null hypothesis). It is also possible to combine random effects with selection, such as with the Ornstein-Uhlenbeck (OU) model (Butler and King, 2004). This model predicts patterns expected when morphology deviates from neutral evolution by evolving to adaptive optima.

In this study we focus in a species complex within *Liolaemus*, the *L. rothi* complex, which includes 6 named species: *L. rothi* (Koslowsky, 1898), *L. sagei* (Etheridge and Christie, 2003), *L. hermannunezi* (Pincheira-Donoso et al., 2007), *L. tromen* (Abdala et al., 2012), *L. sitesi* (Avila et al., 2013), *L. loboi* (Abdala, 2003). It also includes two candidate species (*Eulaemus* subgenus) previously hypothesized by Olave et al. (2014a; *L.* sp. 4) and Morando (2004; *L.* sp. M34). In this study we estimate a time-calibrated, coalescent-based multilocus phylogeny (using 2 mt and 12 nuclear loci) to compare levels of divergence between molecular and morphological traits within the complex, and also test neutral vs. natural selection by evaluating five different models of phenotypic evolution. We compare our species tree with previous studies and discuss the role of natural selection in the phenotypic evolution within the *L. rothi* complex, which could be a contributing factor in "hiding" some of the diversity in *Liolaemus*.

2. Material and methods

2.1. Field sampling

We included a total of 97 terminals representing all described species of the *L. rothi* complex (*L. sagei*, *L. hermannunezi*, *L. tromen*, *L. sitesi*, *L. loboi*, *L. rothi*) collected from all or most of their known distributional ranges, and two candidate species (*L.* sp. 4: Olave et al., 2014a; *L.* sp. M34: Morando, 2004). Note that Olave et al. (2014a) also proposed other species candidate for the *L. rothi* complex, but these species are suspected to be hybrids between *rothi* and *boulengeri* complexes (discussed in the same article Olave et al., 2014a; Olave et al. (in prep.)), thus in a conservative framework, we only included here those individuals not showing mitochondrial introgression with species in the *boulengeri* complex. We also included two outgroup species, *L. inacayali* and *L. senguer*. Specimens were collected by hand or noose, sacrificed by a pericardiac injection of sodium tiopenthal (Abbot®/Pentovet®), dissected slightly to extract a sample of liver/muscle for molecular study, fixed in 10–20% formalin, and later transferred to 70% ethanol. Tissues were stored in a freezer with 96% ethanol. Voucher specimens are deposited in the herpetological collections LJAMM-CNP of the Instituto Patagónico para el Estudio de Ecosistemas Continentales (IPEEC), Centro Nacional Patagónico, Puerto Madryn, Argentina (CENPAT–CONICET, http://www.cenpat.edu.ar/nuevo/colecciones03.html), and at the Bean Life Science Museum, Brigham Young University (BYU; http://mlbean.byu.edu/ResearchCollections/Collections/ReptilesandAmphibians.aspx) (Appendix S1, available online).

2.2. Laboratory procedures

We sequenced two mitochondrial genes, four anonymous nuclear loci (ANL) and eight nuclear protein-coding loci (NPCL), a total of 14 genes (10,013 bp). Sequences are deposited in GenBank (Accession Nos. KX865285-KX865595, KX885565-KX885852), and alignments in the Dryad data base (Dryad accession: http://dx.doi.org/10.5061/dryad.3g141). Genomic DNA was extracted using the Qiagen®DNeasy® 96 Tissue Kit following the protocol provided by the manufacturer. For PCR and sequencing protocols we followed Morando et al. (2003) for the mitochondrial genes (cyt-b and 12S), Camargo et al. (2012) for the four anonymous nuclear

loci (ANL: A1D, A12D, A4B and A9C), and eight nuclear protein coding loci (NPCL): EXPH5, KIF24, MXRA5, (Portik et al., 2012), DNAH3, PRLR, PNN, SNCAIP (Townsend et al., 2008), and CMOS (Wiens et al., 1999).

We amplified all nuclear genes using the touchdown PCR cycle described by Noonan and Yoder (2009), with standard reaction conditions (per sample: 2 μl dNTPs (1.25 mM), 2 μl 5x Taq buffer, 1 μl each primer (10 μM), 1 μl MgCl (25 mM), and 0.1 μl Taq DNA polymerase (5 U/μl; Promega Corp., Madison, WI); 14 ml total reaction volume). All sequences were edited using the program Sequencher v4.8. (™Gene Codes Corporation Inc. 2007), and aligned with MAFFT (Katoh et al., 2002) based on 100 tree rebuilding iterations and a maxirate of 100. Protein-coding genes were translated to amino acids to check for codon errors. Missing data in all cases were coded as "?". For each gene we selected the best-fitting model of evolution using JModelTest v0.1.1 (Posada, 2008) using the Akaike Criterion Information (corrected) (AICc). We tested for recombination in all nuclear genes using RDP: Recombination Detection Program v3.44 (Heath et al., 2006).

2.3. Species tree estimation

We included a total of 14 loci and 97 individuals for species tree estimation using the coalescent based program ∗BEAST v1.6 (Heled and Drummond, 2010). The program was run for 100×10^6 MCMC generations (burnin 10%), sampling every 10.000 intervals, and convergence was diagnosed when ESS values > 200.

2.4. Divergence time estimation

We used available mutation rates estimated for *Liolaemus* (Olave et al., 2014a; Table 1) for divergence time estimates, and BEAST v1.6.2 and a strict clock for each gene under a gamma distribution and a Yule prior model. The analysis was run for 100×10^6 MCMC generations (burnin 10%), sampling every 10,000 intervals with convergence diagnosed when ESS values > 200.

2.5. Morphological comparisons

We used a Schwyz electronic digital caliper of 0.1 mm precision to measure nine morphometric variables commonly used to study *Liolaemus* species (see Table S1 for references of previous *Liolaemus* studies). We selected measures to represent total body size and anterior/posterior extremities: snout–vent length (SVL - distance from the tip of the snout and the posterior margin of the precloacal scales.), axilla-groin distance (AGD - distance from the armpit of the right front leg to the anterior insertion of the hind limb), hand length (HaL – distance between the base of the wrist and base of the nail of the third digit; including third measured ventrally), foot length (FoL – distance between the base of the heel to the base of the nail of the fourth digit; measured ventrally), tibio-fibula length (TFL - from knee to the internal angle with the foot), knee-knee distance (KKD - distance between knees bent at right angles to the abdomen, measured ventrally), ratio-ulna length (RUL - from elbow to internal angle with the hand), humerus length (HL - from shoulder to the internal angle of the elbow), femur length (FL – from the hip insertion to the knee). We also registered by eye 15 color pattern variables: vertebral line melanism (VLM, codified as round spots, bands or absence); number of spots at the left vertebral line (NSLVL); number of spots at the right vertebral line (NSRVL); presence of a white spot below VLM spots (PWSVL, codified as presence/absence); paravertebral melanism (PVM, codified as round spot, bands or absence), number of left paravertebral spots (NLPS)); number of right paravertebral spots (NRPS); presence of a white spot below PVM spots (PWSPL, codified as presence/absence); mean line between MLV and MPV (ML, codified as presence/absence); scapular melanism (SM, codified as presence/absence); gular melanism (GM, codified as spots, full melanism or absence); ventral melanism (VM, codified as spots, full melanism or absence); ventral color (ventral color, codified as light or dark); forelimb melanism (FM, codified as presence/absence of spots); hindlimb melanism (HM, codified as presence/absence of spots).

We performed morphological comparisons among species using the R program and including each inferred main clade (C1 and C2, see results). We included a total of nine morphometric variables and 15 color pattern variables for these analyses (Table S1, available online). We first evaluated the utility of each morphometric variable using the non-parametric Kruskal-Wallis test (Kruskal and Wallis, 1952). We then implemented the multivariate MANOVA test and Hotteling contrasts. Following Escudero et al. (2012), color pattern variables were used to construct contingency tables and analyzed using Pearson's χ^2 with 5000 Markov permutations. Because eight of the 15 color pattern variables were used here for the very first time (see Table S1), we first demonstrate their informativeness in separating *Liolaemus* species by comparing all species of the *L. rothi* complex against the two outgroups, *L. incayali* and *L. senguer*. We then performed pairwise comparisons among species of the *L. rothi* complex.

Table 1
Calibration details of mutation rate *priors*. Curve shape for all cases = 1.

Locus	Initial value	Scale
12S	0.006339	0.0090
cyt-b	0.019355	0.0174
C-MOS	0.000879215	0.0012
DNAH3	0.00076162	0.0011
EXPH5	0.0012955	0.0015
KIF24	0.0019021	0.0016
LDA12D	0.0026373	0.0038
LDA1D	0.001765	0.0025
LDA4B	0.0035965	0.0050
LDA9C	0.0017753	0.0025
MXRA5	0.00077525	0.0011
PNN	0.00081714	0.0012
PRLR	0.001322	0.002
SNCAIP	0.0010351	0.0015

2.6. Molecular and morphological species delimitation

Using the program iBPP (Solís-Lemus et al., 2015), we evaluated the presence of independent evolving lineages within the *L. rothi* complex by incorporating both molecular and morphological data. We analyzed these separately as well as in combination to explore both the phylogenetic signal of each and the concordance/discordance between them. The program begins with a guide tree and sequentially collapses internal nodes and calculates the posterior probability of each τ equal or different to 0. The models explored are labeled with 0 and 1 at each node, specifying collapsed or split nodes, respectively; this approach specified alternative models ranging from 111 (four species) to 000 (single species). The search used a reversible MCMC (rjMCMC), with a prior specified from a gamma distribution as τ (branch length) and θ ($=N_e\mu$; where N_e is the population size and μ the mutation rate) for the molecular data, and a σ^2 (variance) and λ (within a between species ratio) for the morphological data. We included a prior distribution of θ and $\tau = G(1, 1000)$, which leads to a mean = 0.001, and left default values of σ^2 and $\kappa = 0$, thus the priors are non-informative and the program estimates them. We fine-tuned values during the analysis to ensure that they oscillated between 0.15 and 0.7 (as recommended in the program manual). We used the inferred ∗BEAST tree as guide tree (see results) and ran the MCMC analysis over 50,000 generations, sampled every 5000 steps (10% burnin), and per-

formed two independent analyses for both large clades recovered here (C1 and C2, see results).

2.7. Morphological evolution

We used the inferred species tree and morphometric variables to quantify morphological evolution using the GEIGER package in R (Harmon et al., 2008), and evaluated a total of five models: Brownian motion (BM), Ornstein-Uhlenbeck (OU), Early-burst (EB), trend and kappa. These models include both neutral evolution and selection (see Box 1 for details), and we used the corrected Akaike Criterion (AICc) to select the best-fit model.

Box 1 Details of models tested to study morphological evolution.

BM Brownian motion model (Felsenstein 1973) assumes the correlation structure among trait values is proportional to the extent of shared ancestry for pairs of species.
OU Ornstein-Uhlenbeck model (Butler and King, 2004) fits a random walk with a central tendency with an attraction strength proportional to the parameter alpha.
EB Early-burst model (Harmon et al., 2010), also known as ACDC (accelerated-decelerated). This model involves exponential changes throw time.
Trend Trend is a diffusion model with linear trend in rates through time (toward larger or smaller rates).
Kappa Kappa is a punctuational (speciational) model of trait evolution (Pagel, 1999), where character divergence is related to the number of speciation events between two species.

3. Results

3.1. Species tree and divergence times

We inferred a species tree that shows two strongly supported clades (C1 and C2, PP = 1; Fig. 1), with an average divergence time of 4.59 mya (95% HDP: 3.08–9.45 mya). Clade C1 has a restricted geographic distribution in northwestern Patagonia (north of Neuquén province, Fig. 2) and includes *L. loboi*, *L. hermannunezi*, *L. tromen* and *L.* sp. M34. Candidate species *L.* sp. M34 is sister to *L. hermannunezi*, but with low statistical support (PP = 0.31), and their divergence is dated 1.48 mya (95% HDP: 0.8–2.51 mya). Clade C2 has a more southern distribution (central-west of Neuquén province and central-west of Río Negro province, Fig. 2) and includes *L. rothi*, *L. sagei*, *L. sitesi* and *L.* sp. 4. *Liolaemus* sp. 4 is inferred as sister lineage of *L. rothi* (PP = 1), and their divergence time is estimated at 1.89 mya (95% HDP: 1.07–3.23 mya).

3.2. Molecular and morphological divergence

The combined analyzes of DNA and morphology with iBPP, estimated PP = 1 for each node in the tree (Fig. 3, numbers above branches; selected model PP [111] = 1), including described species and the two candidate species (*L.* sp. M34 and *L.* sp. 4). When exploring each source of information separately, results of the molecular-only analysis remain unchanged for both C1 and C2 (PP [111] = 1), as well as a morphological-only analysis performed for C2. However, our morphology only analyses inferred lower PP values for two of the three nodes of C1 (Fig. 3, numbers below branches: divergence of *L. hermannunezi* and *L.* sp. M34, and divergence of this clade from *L. loboi*). The model selected still represents a fully split tree, but with lower support: PP [111] = 0.5615.

We performed Kruskal-Wallis test to evaluate the utility of each quantitative variable. We identified significant differences, but also

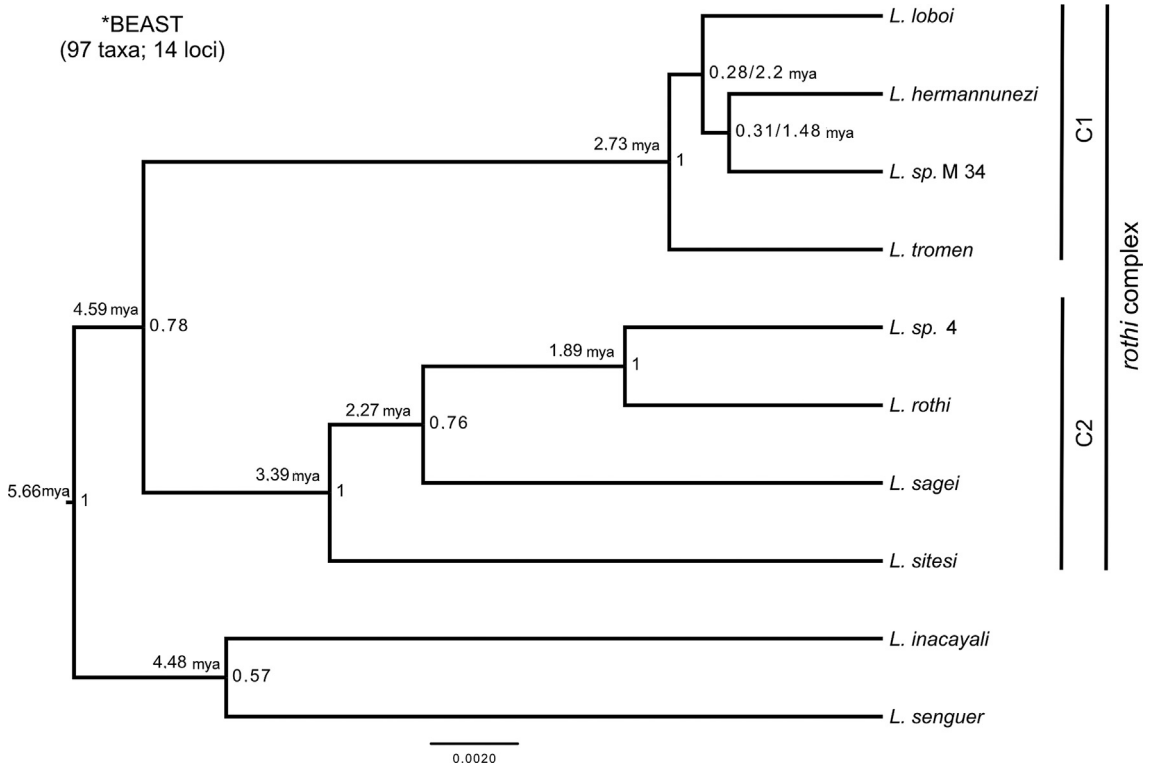

Fig. 1. Species tree estimated for the *L. rothi* complex from 14 loci and 97 individuals. Divergence times and posterior probabilities are shown to the right and left of each node, respectively, except for the two most nested nodes - these estimates are given to the right of each node.

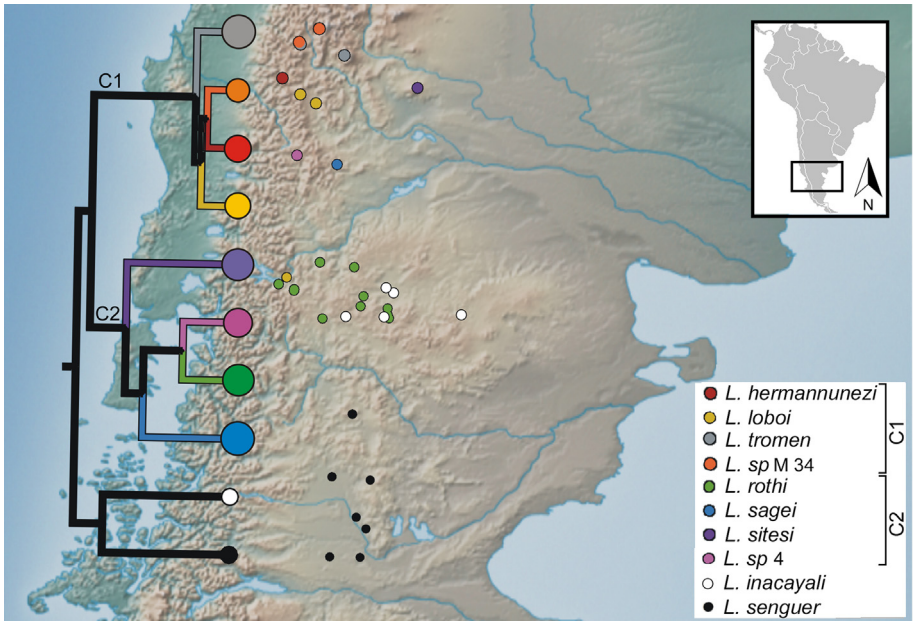

Fig. 2. Species tree projected onto the sampling map for each terminal, with circle sizes scaled to the average SVL of each lineage (Tables 2 and 3).

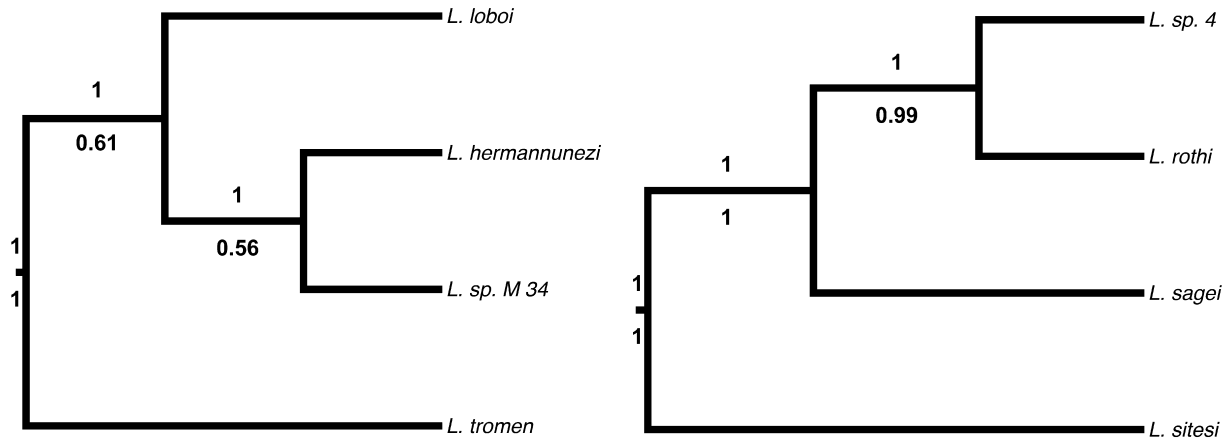

Fig. 3. iBPP results. Posterior probabilities on branches represent analyses based on strict molecular data (above) and morphological traits (below), for C1 (left) and C2 (right).

Table 2
Summary statistics and Hotteling contrast results (alpha = 0.05; df = 98) for quantitative variables for clade C1. Class column represents the group associations.

Species	Variables													n	Class		
	SVL	AGD	HaL	RUL	HL	FoL	TFL	FL	KKD	NSLVL	NSRVL	NLPS	NRPS				
L. tromen	80.7	38.3	11.2	13.3	12.0	20.8	14.9	15.6	34.2	8.0	7.7	7.2	6.7	4	A		
L. hermannunezi	65.2	30.2	10.0	11.4	9.6	18.7	12.9	12.8	29.7	8.2	8.0	8.2	8.0	4		B	
L. sp. M 34	57.1	25.9	9.0	9.5	8.4	16.5	10.9	11.6	25.1	9.3	9.4	8.7	8.6	19		B	
L. loboi	62.8	29.5	9.9	10.3	9.1	18.4	12.1	12.1	27.3	9.7	9.7	8.8	8.7	7			C

Table 3
Summary statistics and Hotteling contrast results (alpha = 0.05; df = 98) for quantitative variables for clade C2. Class column represents the group associations.

Species	Variables													n	Class	
	SVL	AGD	HaL	RUL	HL	FoL	TFL	FL	KKD	NSLVL	NSRVL	NLPS	NRPS			
L. sitesi	76.41	35.18	11.44	13.03	11.13	20.68	14.19	14.73	33.17	10.20	10.00	9.80	9.80	5	A	B
L. rothi	76.47	37.11	12.23	13.72	11.98	21.36	15.14	16.00	33.42	8.21	8.18	7.09	7.03	33	A	
L. sp. 4	69.71	32.16	9.86	11.48	9.85	17.54	12.72	13.15	29.25	9.00	10.00	8.33	9.67	3		B
L. sagei	78.80	35.82	10.86	13.63	11.06	21.32	14.00	16.09	35.03	11.00	10.50	9.50	9.50	2		B

Table 4
χ^2 and p-value calculations for qualitative color patterns variables. Comparison of *L. rothi* complex with outgroups *L. inacayali* and *L. senguer*.

	L. inacayali	*L. senguer*
L. tromen	$\chi^2 = 86.533$, $p = 2 \times 10^{-4}$*	$\chi^2 = 141.69$, $p = 2 \times 10^{-4}$*
L. hermannunezi	$\chi^2 = 45.515$, $p = 0.0012$*	$\chi^2 = 69.156$, $p = 2 \times 10^{-4}$*
L. loboi	$\chi^2 = 37.019$, $p = 0.0073$*	$\chi^2 = 39.521$, $p = 0.0099$*
L. sp. M34	$\chi^2 = 50.184$, $p = 0.0003$*	$\chi^2 = 57.717$, $p = 2 \times 10^{-4}$*
L. sp. 4	$\chi^2 = 23.752$, $p = 0.0203$*	$\chi^2 = 25.074$, $p = 0.0204$*
L. rothi	$\chi^2 = 85.56$, $p = 2 \times 10^{-4}$*	$\chi^2 = 125.35$, $p = 2 \times 10^{-4}$*
L. sagei	$\chi^2 = 24.974$, $p = 0.0065$*	$\chi^2 = 13.503$, $p = 0.0479$*
L. sitesi	$\chi^2 = 37.916$, $p = 0.0039$*	$\chi^2 = 40.743$, $p = 0.0079$*

* Significant differences under 95% confidence.

high overlap among contrast comparisons (Appendix S2, available online). This same result is observed with the MANOVA test: we found significant differences among all lineages ($p < 0.01$, within both clades), but Hotteling contrasts showed overlap between each of the two candidate species (*L.* sp. M34 and *L.* sp. 4) with respect to at least one other species of the same clade (Tables 2 and 3, respectively). *Liolaemus* sp. M34 is assigned to a group "B" shared with *L. hermannunezi* (Table 2), similarly *L.* sp. 4 is assigned to a group "B" shared with *L. sitesi* and *L. sagei* (Table 3).

Our comparisons of color pattern variables between *L. rothi* complex and the two outgroups *L. inacayali* and *L. senguer* were rinferred as significantly different (Table 4). However, when comparing pairs of species within each *L. rothi* complex clade (C1 and C2), we found significant differences only between *L. tromen* and *L. loboi* and *L.* sp. M34; and between *L. sitesi* and *L. rothi* (Tables 5 and 6). All remaining pairwise comparisons showed no significant differences.

3.3. Morphological evolution

Our GEIGER analyses showed that three of nine morphometric variables fit a Brownian model (HaL, FL y KKD), while a trend model is selected for the other six variables (SVL, AGD, RUL, HL, FoL y TFL), indicating linear rate selection (increment and decrement) for most of the variables included here (Table 7). In particular, species included in clade C1 seem to have lower means in snout-vent lengths (SVL, represented in Fig. 2 by circle sizes in terminals) with respect to species in clade C2, the only exception to this is *L. tromen* that showed an average of SVL = 80.8 cm (compared to SVL ranges of C1: 57.1–65.2 cm and C2: 69.71–78.8 cm; Table 2).

4. Discussion

4.1. Hidden diversity in the genus Liolaemus: genetic vs. morphological divergence

We quantified morphological divergence within each of the two main clades inferred in the estimated species tree (C1 and C2; Fig. 1) under traditional multivariate analyses. Results showed overlap of Hotteling groups (Tables 2 and 3), and most pairwise comparisons of color patterns were no-significantly different within clades (Tables 5 and 6). On the other hand, the iBPP analyses of the PP of independent lineages identifies all species (and candidate species) within both clades of the *L. rothi* complex, using both phenotypic and genetic makers in combination or independently (Fig. 3). However, for species included in C1, genetic markers seem to diverge at higher rates than morphological characters; the anal-

Table 5
χ^2 and p-values obtained for contingency table in pairwise comparisons for species in C1.

	L. sp 4	*L rothi*	*L. sagei*
L. rothi	$\chi^2 = 20.311$, $p = 0.6199$		
L. sagei	$\chi^2 = 14.167$, $p = 0.7427$	$\chi^2 = 23.867$, $p = 0.4073$	
L. sitesi	$\chi^2 = 22.151$, $p = 0.2633$	$\chi^2 = 56.672$, $p = 0.0007$*	$\chi^2 = 16.52$, $p = 0.6061$

* Significant differences under 95% confidence.

Table 6
χ^2 and p-values obtained for contingency table in pairwise comparisons for species in C2.

	L. tromen	*L. hermannunezi*	*L. loboi*
L.hermanunnezi	$\chi^2 = 24.132$, $p = 0.3443$		
L. loboi	$\chi^2 = 41.873$, $p = 0.0016$*	$\chi^2 = 14.129$, $p = 0.9090$	
L. sp. M34	$\chi^2 = 89.522$, $p = 2 \times 10^{-4}$*	$\chi^2 = 35.285$, $p = 0.0527$	$\chi^2 = 22.079$, $p = 0.4709$

* Significant differences under 95% confidence.

Table 7
AICc morphological evolution results. Selected models are shown in asterisk for each variable.

Variables	Models				
	BM	OU	EB	Trend	Kappa
SVL	94.81	84.26	84.32	83.80*	84.05
AGD	74.28	69.46	69.48	69.34*	69.48
HaL	30.55*	34.83	34.83	34.83	34.83
RUL	46.85	47.03	47.06	46.78*	47.06
HL	44.88	44.38	44.40	44.19*	44.40
FoL	66.78	53.39	53.41	53.22*	53.41
TFL	50.16	47.94	47.96	47.75*	47.96
FL	45.67*	48.71	48.71	48.70	48.71
KKD	64.53*	65.66	65.69	65.45	65.67

ysis of phenotypic traits alone showed a decrease in PP estimates (PP[111] = 0.5619).

The most recent species divergence within the *L. rothi* complex was dated 1.48 mya (95% HDP = 0.8–2.51 mya; between *L.* M34 and *L. hermannunezi*; Fig. 1); splits of the remaining species are older (1.89–3.39 mya). Although other *Liolaemus* species have acquired subtle but detectable morphological differences over this or more recent divergence times (e.g., Medina et al., 2013, 2014 for the *L. buergeri* complex;), the *L. rothi* complex shows a different pattern, with low PP estimated by iBPP and/or extensive overlap among Hotteling groups of genetically distinct lineages and no differences in most cases of color patterns comparisons. Our tests of phenotypic evolution under the null (Brownian) model vs. alternatives (various modes of selection) detected significant linear changes (trend model) in rates of morphological evolution in six of nine variables evaluated. These tests also revealed differences between clades in rates of evolution for some morphological characters: northern C1 clade species show stasis for smaller body sizes than C2 clade species (Fig. 2).

Adaptation by conserved body size is a plausible explanation for these two clades. Body size is a fundamental character in animal biology that may covary with ecological, physiological, or other life history traits (fecundity, age at maturity, metabolic efficiency, and thermoregulation; Sookias et al., 2012). Thus, body size has complex interactions with fitness (LaBarbera, 1989). For example, larger size could increase success in obtaining food, defending a home range, and reproduction success (Hone and Benton, 2005), against trade-offs with cuckoldry or predation. In this case, species from clade C1 are restricted to higher elevations of the Andean cordillera and pre-cordillera. For example, the type locality of *L. hermannunezi* is located on the Argentina-Chile border at an altitude and latitude (37°31′S; 71°14′W) characterized by strong winds and low temperatures (Garreaud, 2009). Thus clade C1 species may, under strong selection, conserve smaller body sizes at or near an adaptive optimum. Although it would be important to explicitly test this point using ecological and physiological data in future studies, the evidence presented here could represent an important clue to understanding much of the diversity of the genus, and continued study of other species complexes based on multiple data sources in integrative evolutionary frameworks will clarify many details of the larger radiation of this clade.

4.2. The L. rothi complex species tree

Previous studies have proposed different phylogenetic hypotheses for the *L. rothi* complex, but they were based on smaller sample sizes and/or fewer loci. For example, Abdala (2007) made the first inferences under a parsimony framework based on mtDNA and morphological traits in a concatenated matrix. More recently Avila et al. (2013) included a Bayesian concatenated analysis of the same 14 loci included here, in the description of a new species, and Olave et al. (2014a) presented the first multilocus coalescent species tree for a large number of species of the subgenus *Eulaemus*, including all described species of the *L. rothi* complex. In this study we report differences in and congruence with our results and these previous studies. For example, Abdala et al. (2012) inferred *L. tromen* nested within the *fitzingeri* clade using morphological characters, but other studies using DNA have inferred *L. tromen* within the *L. rothi* complex (Avila et al., 2013; Olave et al., 2014a; and this study). On the other hand, here we inferred two main clades within the *L. rothi* complex (C1 and C2; Fig. 1), with northern and southern distributions and divergences dated 2.73 and 3.39 mya, respectively, which is congruent with Olave et al. (2014a; their Fig. 4). Although the support for these two groups is not high (PP = 0.78), coalescent-based methods generally estimate lower nodal PP values compared to concatenated matrices; the former accommodate conflicting signals among gene trees and down-weight support for those nodes, while concatenated analyses tend to inflate nodal support (e.g., Belfiore et al., 2008; Olave et al., 2014a, 2015). Because multilocus species trees accommodate coalescent processes (Knowles, 2009; Knowles and Kubatko, 2010), they may be more accurate than single gene trees or multilocus concatenated matrices (Leaché and Rannala, 2011).

Fontanella et al. (2012) dated the origin of the *L. rothi* complex at 3.04 mya, but this estimate was based on four loci and only two species representing the group. Our divergence time estimates date the origin of the *L. rothi* complex to the late Pliocene (4.59 mya; Fig. 1); we consider this the more accurate estimate to date given our more complete sampling of individuals and loci (Corl and Ellegren, 2013). We also found statistical support for two new species within the *L. rothi* complex (*L.* sp. 4 and *L.* M34; Fig. 3), based on combining different sources of information that resolved higher PP values for recognition of these two species. New studies have highlighted the risk of delimiting species with single data sources (Edwards and Knowles, 2014; Olave et al., 2014b; Solís-Lemus et al., 2015; Pyron et al., 2016; Huang and Knowles, 2016), and we suggest further exploration of multiple data sets analyzed in an integrative model-based framework (in contrast to an "iterative" taxonomy (Yeates et al., 2011)). More recent studies are incorporating "Next Generation" data into species delimitation (Pyron et al., 2016), and we suggest that options are available now to extend morphological data collection and analyses to include binary, meristic, and geometric morphometric variables (Aguilar et al., 2013), as well as quantification of color (McKay et al., 2014).

Acknowledgments

We thank all members of the Grupo de Herpetología Patagónica (CENPAT-CONICET) for continuing support. Financial support was provided by grants PICT 2006-506 ANPCYT-FONCYT (LJA), ANPCYT-FONCYT 33789 (MM), and a doctoral and postdoctoral fellowship (MO) from Consejo Nacional de Investigaciones Científicas y Técnicas (CONICET), the Kennedy Center for International Studies, the Department of Biology and the M.L. Bean Life Science Museum of BYU, and NSF-PIRE award (OISE 0530267) for support of collaborative research on Patagonian Biodiversity granted to the following institutions (listed alphabetically): Brigham Young University, Centro Nacional Patagónico (AR), Dalhousie University, Instituto Botánico Darwinion (AR), Universidad Austral de Chile, Universidad de Concepción, Universidad Nacional del Comahue, Universidad Nacional de Córdoba, and University of Nebraska. Some financial and logistical support was provided to LJA and MM by NSF award EF – 1241885 to J.W. Sites, Jr.

Appendix S1. Supplementary material

Supplementary data associated with this article can be found, in the online version, at http://dx.doi.org/10.1016/j.ympev.2016.09.009 and Dryad data base: http://dx.doi.org/10.5061/dryad.3g141.

References

Abdala, C.S., 2003. Cuatro nuevas especies del género *Liolaemus* (Iguania: Liolaemidae), pertenecientes al grupo boulengeri, de la Patagonia, Argentina. Cuadernos de Herpetología 17.

Abdala, C.S., 2007. Phylogeny of the *boulengeri* group (Iguania: Liolaemidae, *Liolaemus*). Zootaxa 1538, 1–84.

Abdala, C.S., Semhan, R.V., Moreno Azocar, L., Bonino, M., Paz, M.M., Cruz, F., 2012. Taxonomic study and morphology based phylogeny of the patagonic clade *Liolaemus melanops* group (Iguania: Liolaemidae), with the description of three new taxa. Zootaxa 3163, 1–32.

Abdala, C.S., Quinteros, A.S., 2014. Los últimos 30 años de estudios de la familia de lagartijas más diversa de Argentina. Actualización taxonómica y sistemática de Liolaemidae. Cuadernos de Herpetología 28, 1–28.
Aguilar, C. et al., 2013. Integrative taxonomy and preliminary assessment of species limitis in the Liolaemus walker complex (Squamata, Liolaemidae) with descriptions of three new species from Peru. ZooKeys 364, 47–91.
Avila, L.J., Morando, M., Sites Jr., J.W., 2006. Congeneric phylogeography: hypothesizing species limits and evolutionary processes in Patagonian lizards of the *Liolaemus boulengeri* group (Squamata: Liolaemini). Biol. J. Linn. Soc. 89, 241–275.
Avila, L.J., Olave, M., Perez, C.H.F., Perez, D.R., Morando, M., 2013. Molecular phylogenetic relationships of the *Liolaemus rothi* complex and a new species of lizard from Auca Mahuida Volcano (Squamata: Liolaemini). Zootaxa 3608, 221–238.
Belfiore, N.M., Liang, L., Moritz, C., 2008. Multilocus phylogenetics of a rapid radiation in the genus *Thomomys* (Rodentia: Geomyidae). Syst. Biol. 57, 294–310.
Breitman, M.F., Avila, L.J., Sites Jr., J.W., Morando, M., 2011. Lizards from the end of the world: phylogenetic relationships of the *Liolaemus lineomaculatus* section (Squamata: Iguania: Liolaemini). Mol. Phylogenet. Evol. 59, 364–376.
Breitman, M.F., Avila, L.J., Sites Jr., J.W., Morando, M., 2012. How lizards survived blizzards: phylogeography of the *Liolaemus lineomaculatus* group (Liolaemidae) reveals multiple breaks and refugia in southern Patagonia, and their concordance with other co-distributed taxa. Mol. Ecol. 25, 6068–6085.
Butler, M.A., King, A., 2004. Phylogenetic comparative analysis: a modeling approach for adaptive evolution. Am. Nat. 164, 683–695.
Camargo, A., Avila, L.J., Morando, M., Sites Jr., J.W., 2012. Accuracy and precision of species trees: effects of locus, individual and base pair sampling on inference of species trees in lizards of the *Liolaemus darwinii* Group (Squamata, Liolaemidae). Syst. Biol. 61, 272–288.
Camargo, A., Sites Jr., Jack, 2013. Species Delimitation: A Decade After the Renaissance. INTECH Open Access Publisher.
Carstens, B.C., Pelletier, T.A., Reid, N.M., Salter, J.D., 2013. How to fail at species delimitation. Mol. Ecol. 22, 4369–4383.
Corl, A., Ellegren, H., 2013. Sampling strategies for species trees: the effects on phylogenetic inference of the number of genes, number of individuals, and whether loci are mitochondrial, sex-linked, or autosomal. Mol. Phylogenet. Evol. 67, 358–366.
De Queiroz, K., 2007. Species concepts and species delimitation. Syst. Biol. 56, 879–886.
Edwards, D.L., Knowles, L.L., 2014. Species detection and individual assignment in species delimitation: can integrative data increase efficacy? Proc. R. Soc. B. http://dx.doi.org/10.1098/rspb.2013.2765 20132765.
Escudero, P.C., Minoli, I., Frutos, N., Avila, L.J., Morando, M., 2012. Estudio comparativo del melanismo en lagartijas del grupo Liolaemus fitzingerii (Liolaemini: Liolaemus). Cuadernos de herpetología 26.
Etheridge, R., Christie, M.I., 2003. Two new species of the lizard genus *Liolaemus* (Squamata: Liolaemidae) from northern Patagonia, with comments on Liolaemus rothi. J. Herpetol. 37, 325–341.
Fontanella, F.M., Olave, M., Avila, L.J., Sites Jr., J.W., Morando, M., 2012. Molecular dating and diversification of the South American lizard genus *Liolaemus* (subgenus *Eulaemus*) based on nuclear and mitochondrial DNA sequences. Zool. J. Linnean Soc. 164, 825–835.
Garreaud, R.D., 2009. The Andes climate and weather. Adv. Geosci. 7, 1–9.
Harmon, L.J., Weir, J., Brock, C., Glor, R.E., Challenger, W., 2008. GEIGER: investigating evolutionary radiations. Bioinformatics 24, 129–131.
Harmon, L.J., Losos, J.B., Jonathan Davies, T., Gillespie, R.G., Gittleman, J.L., Bryan Jennings, W., Kozak, K.H., McPeek, M.A., Moreno-Roark, F., Near, T.J., Purvis, A., Ricklefs, R.E., Schluter, D., Schulte II, J.A., Seehausen, O., Sidlauskas, B.L., Torres-Carvajal, O., Weir, J.T., Mooers, A.Ø., 2010. Early bursts of body size and shape evolution are rare in comparative data. Evol. 64 (8), 2385–2396.
Heath, L., van der Walt, E., Varsani, A., Martin, D.P., 2006. Recombination patterns in aphthoviruses mirror those found in other picornaviruses. J. Virol. 80, 11827–11832.
Heled, J., Drummond, A.J., 2010. Bayesian inference of species trees from multilocus data. Mol. Biol. Evol. 27, 570–580.
Hone, D.W.E., Benton, M.J., 2005. The evolution of large size: how does Cope's rule work? Trends Ecol. Evol. 20, 4–6.
Huang, J.P., Knowles, L., in press. The species versus subspecies conundrum: quantitative delimitation from integrating multiple data types within a single Bayesian approach in Hercules beetles. Syst. Biol. (In press)
Katoh, K., Misawa, K., Kuma, K., Miyata, T., 2002. MAFFT: a novel method for rapid multiple sequence alignment based on fast Fourier transform. Nucleic Acids Res. 30, 3059–3066.
Knowles, L.L., 2009. Statistical phylogeography. Annu. Rev. Ecol. Evol. Syst. 40, 593–612.
Knowles, L.L., Kubatko, L.S., 2010. Estimating Species Trees: Practical and Theoretical Aspects. Wiley, Blackwell.
Koslowsky, J., 1898. Enumeración sistemática y distribución geográfica de los reptiles argentinos. Revista del Museo de La Plata 8, 161–200.
Kruskal, W.H., Wallis, W.A., 1952. Use of ranks in one-criterion variance analysis. J. Am. Stat. Assoc. 47, 583–621.
LaBarbera, M., 1989. Analyzing body size as a factor in ecology and evolution. Annu. Rev. Ecol. Syst. 20, 97–117.
Leaché, A.D., Rannala, B., 2011. The accuracy of species tree estimation under simulation: a comparison of methods. Syst. Biol. 60, 126–137.
McKay, B.D. et al., 2014. Incorporating color into integrative taxonomy: analysis of the varied tit (*Sittiparus varius*) complex in East Asia. Syst. Biol. 63, 505–517.
Medina, C.D., Avila, L.J., Morando, M., 2013. Hacia una taxonomia integral: poniendo a prueba especies candidatas relacionadas a *Liolaemus buergeri* Werner 1907 (Iguania: Liolaemini) mediante análisis morfológicos. Cuadernos de Herpetologia 27, 27–34.
Medina, C.D., Avila, L.J., Sites, J.W., Morando, M., 2014. Multilocus phylogeography of the Patagonian lizard complex *Liolaemus kriegi* (Iguania: Liolaemini). Biol. J. Linn. Soc. 113, 256–269.
Morando, M., Avila, L.J., Sites Jr., J.W., 2003. Sampling strategies for delimiting species: genes, individuals, and populations in the Liolaemus elongatus–kriegi complex (Squamata: Liolaemidae) in Andean-Patagonian South America. Syst. Biol. 52, 159–185.
Morando, M., 2004. Sistemática y filogenia de grupos de especies de los géneros *Phymaturus* y *Liolaemus* (Squamata: Tropiduridae: Liolaeminae) del oeste y sur de Argentina (Unpublished D. Phil. Thesis). Universidad Nacional de Tucumán, Argentina.
Morando, M., Avila, L.J., Baker, J., Sites Jr., J.W., 2004. Phylogeny and phylogeography of the *Liolaemus darwinii* complex (Squamata: Liolaemidae): evidence for introgression and incomplete lineage sorting. Evolution 58, 842–861.
Morando, M., Avila, L.J., Turner, C., Sites Jr., J.W., 2007. Molecular evidence for species complex in the Patagonian lizard *Liolaemus bibronii* and phylogeography of the closely related *Liolaemus gracilis* (Squamata: Liolaemini). Mol. Phylogenet. Evol. 43, 952–973.
Morando, M., Avila, L.J., Turner, C., Sites Jr., J.W., 2008. Phylogeography between valleys and mountains: the history of *Liolaemus koslowskyi* (Squeamata, Liolaemini). Zoolog. Scr. 37, 603–638.
Noonan, B., Yoder, A.D., 2009. Anonymus nuclear markers for Malagasy plated lizards (*Zonosaurus*). Mol. Ecol. Resour. 9. 402–404.
Olave, M., Avila, L.J., Sites Jr., J.W., Morando, M., 2014a. A. Multilocus phylogeny of the widely distributed South American lizard clade *Eulaemus* (Liolaemini, *Liolaemus*). Zoolog. Scr. http://dx.doi.org/10.1111/zsc.12053.
Olave, M., Sola, E., Knowles, L.L., 2014b. B. Upstream analyses create problems with DNA-based Bayesian species delimitation. Syst. Biol. 63, 263–271.
Olave, M., Avila, L.J., Sites Jr., J.W., Morando, M., 2015. Model-based approach to test hard polytomies in the *Eulaemus* clade of the most diverse South American lizard genus *Liolaemus* (Liolaemini, Squamata). Zool. J. Linnean Soc. 174, 169–184.
Pagel, M., 1999. Inferring the historical patterns of biological evolution. Nature 401, 877–884.
Pincheira-Donoso, D., Scolaro, J.A., Schulte, J.A., 2007. The limits of polymorphism in Liolaemus rothi: molecular and phenotypic evidence for a new species of the Liolaemus boulengeri clade (Iguanidae, Liolaemini) from boreal Patagonia of Chile. Zootaxa 1452, 25–42.
Portik, D., Wood Jr., P.L., Grismer, J.L., Stanley, E.L., Jackman, T.R., 2012. Identification of 104 rapidly-evolving nuclear protein-coding markers for amplification across scaled reptiles using genomic resources. Conservation Genetic Resour. 4, 1–10.
Posada, D., 2008. JModelTest: phylogenetic model averaging. Mol. Biol. Evol. 25, 1253–1256.
Pyron, R.A., Hsieh, F., Lemmon, A.R., Lemmon, E.M., Hendry, C.R., 2016. Integrating phylogenomic and morphological data to assess candidate species-delimitation models in brown and red-bellied snakes (*Storeria*). Zool. J. Linnean Soc. http://dx.doi.org/10.1111/zoj.12392.
Rannala, B., Yang, Z., 2013. Improved reversible jump algorithms for Bayesian species delimitation. Genetics 194, 245–253.
Solís-Lemus, C., Knowles, L.L., Ané, C., 2015. Bayesian species delimitation combining multiple genes and traits in a unified framework. Evolution 69, 492–507.
Sookias, R.B., Butler, R.J., Benson, R.B.J., 2012. Rise of dinosaurs reveals major body-size transitions are driven by passive processes of trait evolution. Proc. R. Soc. London B 279, 2180–2187.
Townsend, T.M., Alegre, R.E., Kelley, S.T., Wiens, J.J., Reeder, T.W., 2008. Rapid developmental of multiple nuclear loci for phylogenetic analysis using genomic resources: an example from squamate reptiles. Mol. Phylogenet. Evol. 47, 129–142.
Wiens, J.J., Reeder, T.W., Montes de Oca, A.N., 1999. Molecular phylogenetics and evolution in sexual dichromatism among population of the Yarrow's spiny lizard (*Sceloporus jarrovii*). Evolution 53, 1884–1897.
Yang, Z., Rannala, B., 2010. Bayesian species delimitation using multilocus sequence data. Proc. Natl. Acad. Sci. U.S.A. 107, 9264–9269.
Yeates, D.K., Seago, A., Nelson, L., Cameron, S.L., Joseph, L., Trueman, J.W.H., 2011. Integrative taxonomy, or iterative taxonomy? Syst. Entomol. 36, 209–217.